Further study of the $N\Omega$ dibaryon within constituent quark models

Hongxia Huang,[1] Jialun Ping,[1,*] and Fan Wang[2]
[1]*Department of Physics and Jiangsu Key Laboratory for Numerical Simulation of Large Scale Complex Systems, Nanjing Normal University, Nanjing 210023, People's Republic of China*
[2]*Department of Physics, Nanjing University, Nanjing 210093, People's Republic of China*
(Received 23 September 2015; published 3 December 2015)

Inspired by the discovery of the dibaryon d^* and the experimental search of $N\Omega$ dibaryon with the STAR data, we study the strange dibaryon $N\Omega$ further in the framework of the quark delocalization color screening model and the chiral quark model. We have shown $N\Omega$ is a narrow resonance in $\Lambda\Xi$ D-wave scattering before. However, the $\Lambda - \Xi$ scattering data analysis is quite complicated. Here we calculate the low-energy $N\Omega$ scattering phase shifts, scattering length, effective range, and binding energy to provide another approach of STAR data analysis. Our results show there exists an $N\Omega$ "bound" state, which can be observed by the $N - \Omega$ correlation analysis with RHIC and LHC data, or by the new developed automatic scanning system at J-PARC. In addition, we also find that the hidden-color channel coupling is important for the $N\Omega$ system to develop intermediate-range attraction.

DOI: 10.1103/PhysRevC.92.065202   PACS number(s): 13.75.Cs, 12.39.Pn, 12.39.Jh, 24.85.+p

I. INTRODUCTION

The possible existence of dibaryon states was first proposed by Dyson and Xuong [1] in 1964. However, this topic got considerable attention only after Jaffe's prediction of the H particle in 1977 [2]. All quark models, lattice QCD calculations, and other methods, predict that in addition to $q\bar{q}$ mesons and q^3 baryons, there should be multiquark systems: $(q\bar{q})^2, q^4\bar{q}, q^6$, quark-gluon hybrids $q\bar{q}g, q^3g$, and glueballs [3]. A worldwide theoretical and experimental effort to search for dibaryon states with and without strangeness has lasted a long time already.

Recently, an $IJ^P = 03^+$ deep bond $\Delta\Delta$ resonance, called d^* in 1989 [4], with a resonance mass $M = 2.37$ GeV and a width $\Gamma \approx 70$ MeV was experimentally confirmed by the WASA-at-COSY Collaboration [5–7]. This "inevitable" dibaryon was extensively studied in our group [4,8,9]. For its narrow decay width, the phase space reduction and hidden color effect are the possible explanation in the quark model [10–12]. In addition, the mass and the small width of this resonance have been explained by the purely hadronic model (no quarks) of Gal and Garcilazo [13,14]. To provide more theoretical input for experimental search, we included $IJ^P = 03^+$ $\Delta\Delta$ channel coupling to the NN D-wave scattering phase shift calculation and a resonance at $E_{\mathrm{c.m.}} = 2.36$ MeV was shown in [10] which called for the precise pn scattering measurement. Based on the fitting of our model to the NN and YN interaction data our research was also extended to dibaryons with strangeness; several strange dibaryon resonances were shown in specific baryon-baryon channels [15,16], among which the most interesting one is the $N\Omega$ state, a very narrow resonance in $\Lambda\Xi$ D-wave scattering.

In 1987, Goldman *et al.* proposed that the $S = -3, I = 1/2, J = 2$ dibaryon state $N\Omega$ might be a narrow resonance in a relativistic quark model [17]. The quark delocalization color screening model (QDCSM) confirmed that it was a very narrow resonance [15], whereas the chiral quark model also claimed that $N\Omega$ might be a bound state [18]. Recently, the interest in the $N\Omega$ dibaryon was revived by lattice QCD calculations of HAL QCD Collaboration [19]. They reported that the $N\Omega$ is indeed a bound state at pion mass 875 MeV. To search for $N\Omega$ dibaryon experimentally through the D-wave $\Lambda\Xi$ scattering process is complicated, as neither Λ nor Ξ is a stable particle, Ξ decays to $\Lambda\pi$, and Λ decays to $p\pi$. Because N is stable, it is possible to observe $N\Omega$ scattering experimentally. To provide more choices for experimental search, here we calculate the low-energy scattering phase shifts, scattering length, effective range, and the binding energy of the $N\Omega$ system. If it is a sharp resonance, it could be observed by relativistic heavy-ion collision data obtained at RHIC and LHC, or by the hadron beam experiments at J-PARC with their new developed automatic scanning system [20].

Quantum chromodynamics (QCD) was verified to be the fundamental theory of the strong interaction in the perturbative region. However, in the low-energy region, it is hard to directly use QCD to study the complicated systems such as hadron-hadron interactions and multiquark states because of the nonperturbative complication, although lattice QCD has made impressive progresses on nucleon-nucleon (NN) interactions and tetra- and penta-quark systems [21–23]. Therefore, various QCD-inspired models have been developed to get physical insights into the multiquark systems.

To study the baryon-baryon interaction, the most common approach is the chiral quark model (ChQM) [24,25], in which the constituent quarks interact with each other through colorless Goldstone boson exchange in addition to the colorful one-gluon exchange and confinement. To obtain the immediate-range attraction of NN interaction, the chiral partner σ-meson exchange has to be introduced. Although the σ meson, as $\pi\pi$ S-wave resonance, was observed by BES collaboration [26], the calculation of the nuclear force with correlated $\pi\pi$ exchange could not obtain enough attraction [27] as the phenomenological σ-meson exchange did.

*jlping@njnu.edu.cn

An alternative approach to study baryon-baryon interaction is the quark delocalization color screening model (QDCSM), which was developed in the 1990s with the aim of explaining the similarities between nuclear and molecular forces [28]. The model gives a good description of NN and YN interactions and the properties of deuteron [9,29]. It is also employed to calculate the baryon-baryon scattering phase shifts in the framework of the resonating group method (RGM), and the dibaryon candidates are also studied with this model [10,16]. Recent studies also show that the NN intermediate-range attraction mechanism in the QDCSM, quark delocalization, and color screening, is equivalent to the σ-meson exchange in the chiral quark model, and the color screening is an effective description of the hidden-color channel coupling [30,31].

So it is interesting to do a comparative study of the $N\Omega$ system with these two quark models. This state might serve as a test of the flavor-dependent $q-q$ interaction from Goldstone-boson exchange and from quark delocalization color screening, because there is no common flavor quark between N and Ω and so no quark exchange between these two baryons.

The structure of this paper is as follows. A brief introduction of constituent quark models used is given in Sec. II. Section III devotes to the numerical results and discussions. The summary is shown in the last section.

II. TWO QUARK MODELS

To estimate the model dependence of dibaryon prediction, the two quark models, ChQM and QDCSM, are employed here to study the $N\Omega$ system.

A. Chiral quark model

The Salamanca model was chosen as the representative of the chiral quark models, because the Salamanca group's work covers the hadron spectra, nucleon-nucleon interaction, and multiquark states. In this model, the constituent quarks interact with each other through Goldstone-boson exchange and one-gluon exchange in addition to the color confinement. The model details can be found in Ref. [25]. Here we only give the Hamiltonian:

$$H = \sum_{i=1}^{6}\left(m_i + \frac{p_i^2}{2m_i}\right) - T_{\rm CM} + \sum_{j>i=1}^{6}\left(V_{ij}^C + V_{ij}^G + V_{ij}^\chi + V_{ij}^\sigma\right), \tag{1}$$

$$V_{ij}^C = -a_c \boldsymbol{\lambda}_i^c \cdot \boldsymbol{\lambda}_j^c \left(r_{ij}^2 + v_0\right), \tag{2}$$

$$V_{ij}^G = \frac{1}{4}\alpha_s \boldsymbol{\lambda}_i^c \cdot \boldsymbol{\lambda}_j^c \left[\frac{1}{r_{ij}} - \frac{\pi}{2}\delta(\boldsymbol{r}_{ij})\left(\frac{1}{m_i^2} + \frac{1}{m_j^2} + \frac{4\boldsymbol{\sigma}_i\cdot\boldsymbol{\sigma}_j}{3m_i m_j}\right) - \frac{3}{4m_i m_j r_{ij}^3}S_{ij}\right], \tag{3}$$

$$V_{ij}^\chi = V_\pi(\boldsymbol{r}_{ij})\sum_{a=1}^{3}\lambda_i^a\cdot\lambda_j^a + V_K(\boldsymbol{r}_{ij})\sum_{a=4}^{7}\lambda_i^a\cdot\lambda_j^a + V_\eta(\boldsymbol{r}_{ij})\left[\left(\lambda_i^8\cdot\lambda_j^8\right)\cos\theta_P - \left(\lambda_i^0\cdot\lambda_j^0\right)\sin\theta_P\right], \tag{4}$$

$$V_\chi(\boldsymbol{r}_{ij}) = \frac{g_{\rm ch}^2}{4\pi}\frac{m_\chi^2}{12m_i m_j}\frac{\Lambda_\chi^2}{\Lambda_\chi^2 - m_\chi^2}m_\chi\left\{(\boldsymbol{\sigma}_i\cdot\boldsymbol{\sigma}_j)\left[Y(m_\chi r_{ij}) - \frac{\Lambda_\chi^3}{m_\chi^3}Y(\Lambda_\chi r_{ij})\right] + \left[H(m_\chi r_{ij}) - \frac{\Lambda_\chi^3}{m_\chi^3}H(\Lambda_\chi r_{ij})\right]S_{ij}\right\},$$

$$\chi = \pi, K, \eta, \tag{5}$$

$$V_{ij}^\sigma = -\frac{g_{\rm ch}^2}{4\pi}\frac{\Lambda_\sigma^2}{\Lambda_\sigma^2 - m_\sigma^2}m_\sigma\left[Y(m_\sigma r_{ij}) - \frac{\Lambda_\sigma}{m_\sigma}Y(\Lambda_\sigma r_{ij})\right], \tag{6}$$

$$S_{ij} = \left\{3\frac{(\boldsymbol{\sigma}_i\cdot\boldsymbol{r}_{ij})(\boldsymbol{\sigma}_j\cdot\boldsymbol{r}_{ij})}{r_{ij}^2} - \boldsymbol{\sigma}_i\cdot\boldsymbol{\sigma}_j\right\}, \tag{7}$$

$$H(x) = (1 + 3/x + 3/x^2)Y(x), \quad Y(x) = e^{-x}/x, \tag{8}$$

where α_s is the quark-gluon coupling constant. To cover the wide energy scale from light, strange to heavy quark one introduces an effective scale-dependent quark-gluon coupling constant $\alpha_s(\mu)$ [32],

$$\alpha_s(\mu) = \frac{\alpha_0}{\ln\left(\frac{\mu^2+\mu_0^2}{\Lambda_0^2}\right)}, \tag{9}$$

where μ is the reduced mass of the interacting quark pair. The coupling constant $g_{\rm ch}$ for the chiral field is determined from the $NN\pi$ coupling constant through

$$\frac{g_{\rm ch}^2}{4\pi} = \left(\frac{3}{5}\right)^2\frac{g_{\pi NN}^2}{4\pi}\frac{m_{u,d}^2}{m_N^2}. \tag{10}$$

The other symbols in the above expressions have their usual meanings.

For dibaryon with strangeness, two versions of the chiral quark model [33,34] were used. One is the so-called extended chiral SU(2) quark model, in which σ-meson exchange was used between any quark pair. Another is the chiral SU(3) quark model, where full SU(3) scalar octet meson exchange was used. To analyze the effect of the scalar meson exchange of the ChQM, in this work, we use three kinds of chiral quark models: (1) ChQM1, where σ-meson exchange is universal, i.e., it exchanges between any quark pair; (2) ChQM2, where σ meson is restricted to exchange between u and/or the d quark pair only; (3) ChQM3, where the full SU(3) scalar octet meson exchange is employed. These scalar potentials have the same functional form as the one of SU(2) ChQM but a different SU(3) operator dependence [33], that is,

$$V_{ij}^{\sigma_a} = V_{a_0}(\boldsymbol{r}_{ij})\sum_{a=1}^{3}\lambda_i^a\cdot\lambda_j^a + V_\kappa(\boldsymbol{r}_{ij})\sum_{a=4}^{7}\lambda_i^a\cdot\lambda_j^a + V_{f_0}(\boldsymbol{r}_{ij})\lambda_i^8\cdot\lambda_j^8 + V_\sigma(\boldsymbol{r}_{ij})\lambda_i^0\cdot\lambda_j^0 \quad (11)$$

$$V_k(\boldsymbol{r}_{ij}) = -\frac{g_{\rm ch}^2}{4\pi}\frac{\Lambda_k^2 m_k}{\Lambda_k^2-m_k^2}\left[Y(m_k r_{ij}) - \frac{\Lambda_k}{m_k}Y(\Lambda_k r_{ij})\right],$$

with $k = a_0,\kappa, f_0$ or σ.

B. Quark delocalization color screening model

The Hamiltonian of QDCSM is almost the same as that of the chiral quark model but with two modifications [28,29]: First, there is no scalar meson exchange in QDCSM, and second, the screened color confinement used between quark pairs resides in different baryon orbits. That is,

$$V_{ij}^C = \begin{cases} -a_c\boldsymbol{\lambda}_i^c\cdot\boldsymbol{\lambda}_j^c\left(r_{ij}^2+v_0\right) & \text{if } i,j \text{ in the same baryon orbit} \\ -a_c\boldsymbol{\lambda}_i^c\cdot\boldsymbol{\lambda}_j^c\left(\frac{1-e^{-\mu_{ij}r_{ij}^2}}{\mu_{ij}}+v_0\right) & \text{otherwise}\end{cases}. \quad (12)$$

The color screening constant μ_{ij} in Eq. (12) is determined by fitting the deuteron properties, NN scattering phase shifts, and $N\Lambda,N\Sigma$ scattering cross sections, $\mu_{uu}=0.45,\mu_{us}=0.19$ and $\mu_{ss}=0.08$, which satisfy the relation $\mu_{us}^2=\mu_{uu}*\mu_{ss}$.

The quark delocalization in QDCSM is realized by replacing the left, right centered single Gaussian functions, the single-particle orbital wave function in the usual quark cluster model,

$$\phi_\alpha(\boldsymbol{S_i}) = \left(\frac{1}{\pi b^2}\right)^{\frac{3}{4}} e^{-\frac{(r-S_i/2)^2}{2b^2}}, \qquad \phi_\beta(-\boldsymbol{S_i}) = \left(\frac{1}{\pi b^2}\right)^{\frac{3}{4}} e^{-\frac{(r+S_i/2)^2}{2b^2}}, \quad (13)$$

TABLE I. The parameters of two models: $m_\pi=0.7$ fm^{-1}, $m_k=2.51$ fm^{-1}, $m_\eta=2.77$ fm^{-1}, $m_\sigma=3.42$ fm^{-1}, $m_{a_0}=m_\kappa=m_{f_0}=4.97$ fm^{-1}, $\Lambda_\pi=4.2$ fm^{-1}, $\Lambda_K=5.2$ fm^{-1}, $\Lambda_\eta=5.2$ fm^{-1}, $\Lambda_\sigma=4.2$ fm^{-1}, $\Lambda_{a_0}=\Lambda_\kappa=\Lambda_{f_0}$=5.2 fm^{-1}, $g_{\rm ch}^2/(4\pi)=0.54$, $\theta_p=-15^0$.

	QDCSM	ChQM1	ChQM2	ChQM3
b (fm)	0.518	0.518	0.518	0.518
m_u (MeV)	313	313	313	313
m_d (MeV)	313	313	313	313
m_s (MeV)	573	573	536	573
a_c (MeV)	58.03	48.59	48.59	48.59
μ_{uu} (fm^{-2})	0.45	–	–	–
μ_{us} (fm^{-2})	0.19	–	–	–
μ_{ss} (fm^{-2})	0.08	–	–	–
v_0 (MeV)	−1.2883	−1.2145	−1.2145	−0.961
α_0	0.510	0.510	0.510	0.583
Λ_0 (fm^{-1})	1.525	1.525	1.525	1.616
μ_0 (MeV)	445.808	445.808	445.808	422.430

TABLE II. The masses of ground-state baryons (in MeV).

	N	Δ	Λ	Σ	Σ^*	Ξ	Ξ^*	Ω
QDCSM	939	1232	1124	1238	1360	1374	1496	1642
ChQM1	939	1232	1124	1239	1360	1376	1498	1644
ChQM2	939	1232	1137	1245	1376	1375	1506	1620
ChQM3	939	1232	1123	1267	1344	1398	1475	1625
Expt.	939	1232	1116	1193	1385	1318	1533	1672

with delocalized ones,

$$\psi_\alpha(\boldsymbol{S_i},\epsilon) = (\phi_\alpha(\boldsymbol{S_i})+\epsilon\phi_\alpha(-\boldsymbol{S_i}))/N(\epsilon),$$
$$\psi_\beta(-\boldsymbol{S_i},\epsilon) = (\phi_\beta(-\boldsymbol{S_i})+\epsilon\phi_\beta(\boldsymbol{S_i}))/N(\epsilon), \quad (14)$$
$$N(\epsilon) = \sqrt{1+\epsilon^2+2\epsilon e^{-S_i^2/4b^2}}.$$

The delocalization parameter $\epsilon(\boldsymbol{S_i})$ is determined by the dynamics of the quark system rather than adjusted parameters. In this way, the system can choose its most favorable configuration through its own dynamics in a larger Hilbert space.

The parameters of these models are given in Table I. The calculated baryon masses in comparison with experimental values are shown in Table II.

III. THE RESULTS AND DISCUSSIONS

Here, we investigate the low-energy properties of the $N-\Omega$ scattering with quantum numbers $S,I,J=-3,1/2,2$ within various constituent quark models mentioned above. The effects of channel coupling are studied carefully, both color-singlet channels (the color symmetry of the $3q$ cluster is [111]) and hidden-color channels (the color symmetry of the $3q$ cluster is [21], which is called the colorful $3q$ cluster) are included in the ChQM. The colorful $3q$ cluster are listed in Table III with color symmetry $[c]$, spin symmetry $[\sigma]$, flavor symmetry $[f]$, isospin I, and strangeness S. The orbital symmetry is limited to be [3]. The labels of all 16 coupled channels of the $N\Omega$ system are listed in Table IV.

To check whether or not there is a bound $N\Omega$ state, a dynamic calculation based on the resonating group method (RGM) [35] was done. Expanding the relative motion wave function between two clusters in the RGM equation by Gaussian bases, the integro-differential equation of RGM reduces to an algebraic equation—a generalized eigenequation. The energy of the system is obtained by solving this generalized eigenequation. In the calculation, the baryon-baryon separation is taken to be less than 6 fm (to keep the

TABLE III. The symmetries of colorful $3q$ cluster.

	N'	Σ'	Ξ'	Λ'	$\Sigma^{*\prime}$	$\Xi^{*\prime}$	Ω'	N''	Σ''	Ξ''	Λ''	Λ_s'
$[c]$	[21]	[21]	[21]	[21]	[21]	[21]	[21]	[21]	[21]	[21]	[21]	[21]
$[\sigma]$	[21]	[21]	[21]	[21]	[21]	[21]	[21]	[3]	[3]	[3]	[3]	[21]
$[f]$	[21]	[21]	[21]	[21]	[3]	[3]	[3]	[21]	[21]	[21]	[21]	[111]
I	$\frac{1}{2}$	1	$\frac{1}{2}$	0	1	$\frac{1}{2}$	0	$\frac{1}{2}$	1	$\frac{1}{2}$	0	0
S	0	1	2	1	1	2	3	0	1	2	1	1

TABLE IV. Channels of the $N\Omega$ system.

1	2	3	4	5	6	7	8
$\Xi^*\Sigma$	$\Xi\Sigma^*$	$\Xi^*\Lambda$	$N\Omega$	$\Xi^*\Sigma^*$	$\Xi''\Sigma^{*\prime}$	$\Xi^{*\prime}\Sigma''$	$\Xi''\Sigma''$
9	10	11	12	13	14	15	16
$\Xi''\Sigma$	$N'\Omega'$	$\Xi^{*\prime}\Lambda''$	$\Xi'\Lambda''$	$\Xi''\Lambda''$	$\Xi''\Lambda'_s$	$\Xi'\Sigma''$	$\Xi''\Lambda'$

TABLE V. The binding energies B with channel coupling.

	B_{sc} (MeV)	B_{5cc} (MeV)	B_{16cc} (MeV)
QDCSM	ub	−6.4	–
ChQM1	−19.6	−48.8	−119.5
ChQM2	ub	ub	−38.3
ChQM3	ub	ub	−13.7

dimensions of matrix manageably small). The binding energies of the $N\Omega$ state in various quark models are listed in Table V, where B_{sc} stands for the binding energy of the single channel $N\Omega$, B_{5cc} means the binding energy with the five color-singlet channels included, and B_{16cc} refers to the binding energy with all the 16 channels coupling.

The single channel calculation shows that the $N\Omega$ is unbound (labelled as "ub" in Table V) in all quark models except the ChQM1, in which a universal σ-meson exchange is used. To show the contribution of each interaction term to the energy of the system, effective potentials between N and Ω are shown in Fig. 1, in which the contributions from various terms, the kinetic energy (V_{vk}), the confinement ($V_{\rm con}$), the one-gluon exchange ($V_{\rm oge}$), the one-boson exchange (V_π, V_K, and V_η), and the scalar octet-meson exchange ($V_\sigma, V_{a_0}, V_\kappa$, and V_{f_0}) are given. For the ChQM, the confinement, the one-gluon exchange does not contribute to the effective potential between N and Ω, because there is no quark exchange between these two baryons; the pion and the a_0 meson do not contribute either because they do not exchange between the $u(d)$ and s quarks. The contributions of other terms to the effective potential are shown in Figs. 1(a)–1(c), in which we can see that the attraction of the $N\Omega$ system mainly comes from the σ-meson-exchange interaction. In ChQM1, the attraction from σ-meson exchange is so large that it leads to a deep attractive potential between the N and Ω, which makes the $N\Omega$ bound. While in ChQM2, where the σ meson is restricted to exchange between the u and d quarks only, there is no σ-meson-exchange interaction between N and Ω. So the total potential is repulsive, resulting in unbound $N\Omega$. In ChQM3, even though the universal σ-meson exchange introduces large attraction, which is canceled by the repulsive potentials of κ and f_0-meson exchange, and also causes the $N\Omega$ unbound.

Things are different in QDCSM. In this model, quark delocalization and color screening work together to provide short-range repulsion and intermediate-range attraction. We illustrate this mechanism by showing contributions of all interaction terms to the effective potential in Fig. 1(d), from which we see that the attraction of the $N\Omega$ system mainly comes from the kinetic energy term because of quark delocalization; other terms provide repulsive potentials, which reduce the total attraction of the $N\Omega$ potential. The single channel approximation of the $N\Omega$ in QDCSM is also unbound as shown in Table V.

Then we consider the effects of channel coupling. From Table V we can see that in ChQM1, the binding energy of the $N\Omega$ increases to 48.8 MeV by including color-singlet

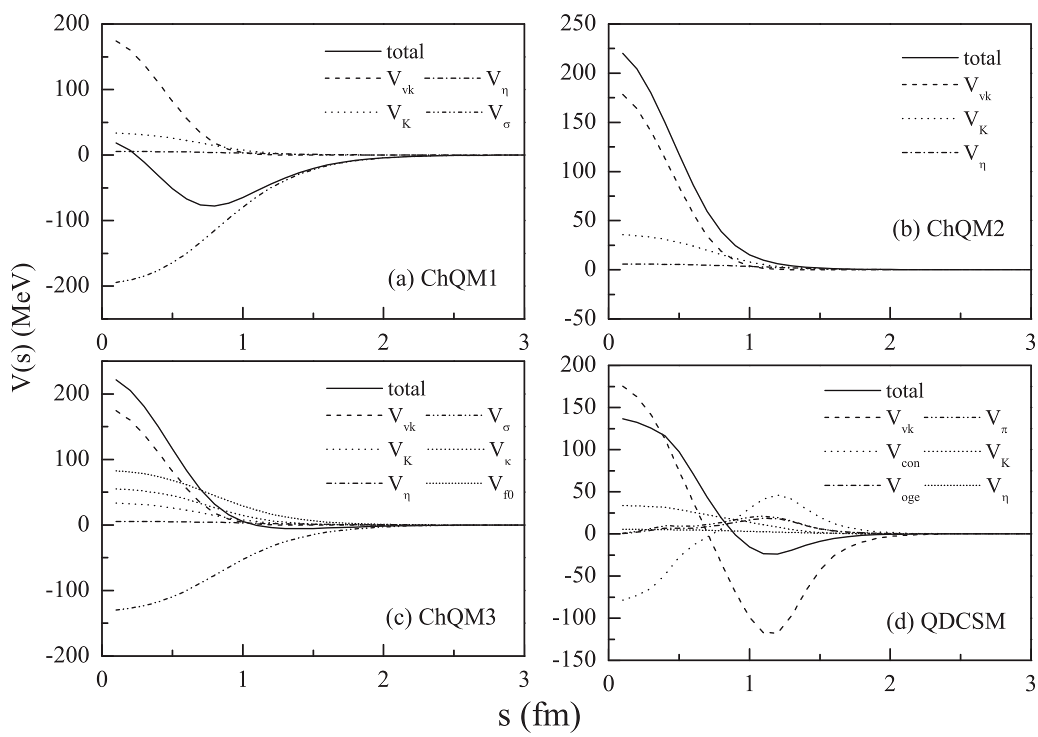

FIG. 1. The contributions to the effective potential from various terms of interactions.

channel coupling, and reaching the largest binding energy of −119.5 MeV with the hidden-color channel coupling, which shows the channel coupling has a huge influence on the $N\Omega$ state. In the ChQM2 and ChQM3, the effect of color-singlet channel coupling is not large enough to make the $N\Omega$ bound; only additional hidden-color channel coupling leads to the bound $N\Omega$ state in both models. In QDCSM, because it contains the hidden-color channel-coupling effect already through the color screening [10,31], including the color-singlet channel coupling only, already makes the $N\Omega$ state bound. All these results are consistent with our previous study of nonstrange channels [10,31], in which we found the QDCSM with color-singlet channel coupling only had similar results as the chiral quark models with both color-singlet and hidden-color channel coupling.

If the $N\Omega$ dibaryon is an S-wave bound state, the strong decays to S-wave octet-decuplet ($\Sigma\Xi^*$, $\Xi\Sigma^*$, and $\Lambda\Xi^*$) and decuplet-decuplet ($\Sigma^*\Xi^*$) channels are prohibited kinematically because its mass will be lower than the thresholds of these channels. It can only decay to the D-wave $\Lambda\Xi$. We had done a scattering calculation by coupling the S-wave $N\Omega$ and the D-wave $\Lambda\Xi$, and found the S-wave bound state $N\Omega$ showed as a resonance in the D-wave $\Lambda\Xi$ scattering process [16]. Because only the tensor interaction can couple the S-wave bound state to the D-wave octet-octet baryon channel, the energy of the bound state is pushed down only a little and the resonance width is generally small. We learned from the Shanghai group of the STAR collaboration that it is quite complicated to analyze the D-wave $\Lambda\Xi$ scattering data because both Λ and Ξ are weak-interaction unstable. To provide more theoretical input, here we calculate the low-energy scattering phase shifts, scattering length, and the effective range of the $N\Omega$ system. All results given below are calculated with 16 channels coupling in the chiral quark models and five color-singlet channels coupling in QDCSM.

First, we calculate the S-wave $N\Omega$ low-energy scattering phase shifts by using the well-developed Kohn-Hulthen-Kato (KHK) variational method. The details can be found in Ref. [35]. Figure 2 illustrates the scattering phase shifts of

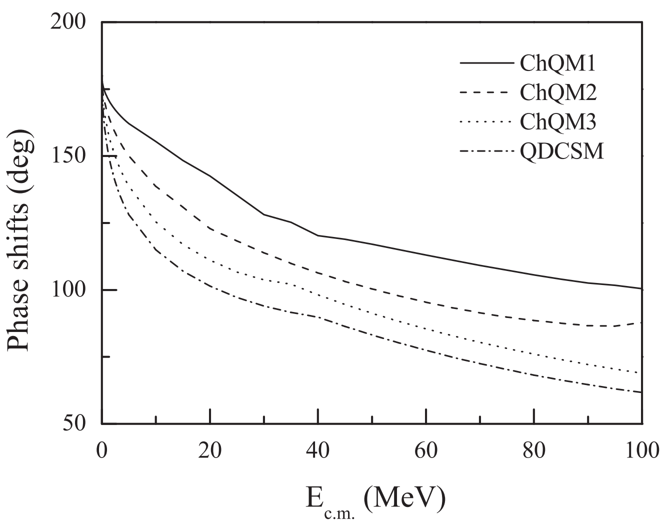

FIG. 2. The phase shifts of S-wave $N\Omega$ dibaryon.

TABLE VI. The scattering length a_0, effective range r_0, and binding energy B' of the $N\Omega$ dibaryon.

	a_0 (fm)	r_0 (fm)	B' (MeV)
QDCSM	2.8007	0.5770	−5.2
ChQM1	0.8103	0.3609	−110.3
ChQM2	1.3808	0.6018	−37.3
ChQM3	1.9870	0.7064	−13.7

the S-wave $N\Omega$. It is obvious that in all four quark models, the scattering phase shifts go to 180° at $E_{\rm c.m.} \sim 0$ and rapidly decreases as $E_{\rm c.m.}$ increases, which implies the existence of a bound state. The results are consistent with the bound state calculation shown before and the lattice QCD calculation [19].

Second, by using these low-energy phase shifts, we extract the scattering length a_0 and the effective range r_0 of $N\Omega$ scattering. Then the binding energy B' is obtained. The scattering length and effective range are calculated from the low-energy scattering phase shifts as

$$k\cot\delta = -\frac{1}{a_0} + \frac{1}{2}r_0k^2 + \mathcal{O}(k^4). \quad (15)$$

The binding energy B' is calculated according to the relation,

$$B' = \frac{\hbar^2\alpha^2}{2\mu}, \quad (16)$$

where μ is the reduced mass of the $N\Omega$; α is the wave number which can be obtained from the relation [36],

$$r_0 = \frac{2}{\alpha}\left(1 - \frac{1}{\alpha a_0}\right). \quad (17)$$

Please note that we use another method to calculate the binding energy, labeled as B'. The results are listed in Table VI.

From Table VI, we can see that in four quark models, the scattering lengths are all positive, which implies the existence of a bound state of $N\Omega$. The binding energies of the $N\Omega$ dibaryon from the two methods (see B and B') are coincident with each other.

IV. SUMMARY

In the quark model, the hadron interaction usually depends critically upon the contribution of the color-magnetic interaction. In this work, we show that for the $N-\Omega$ system with quantum numbers $SIJ = -3\frac{1}{2}2$ the effective interaction has a very small contribution from the color-magnetic interaction because of its special quark content. Because of this, the study of this state might teach us something about the mechanism of the intermediate-range attraction of the baryon-baryon interaction. In the NN case we had shown that the phenomenological σ-meson exchange is equivalent to the quark delocalization and color screening and the latter is an effective description of hidden-color channel coupling. For the $N\Omega$ system, the chiral quark model now only has the Goldstone-boson exchange, which will predict there is not a bound state if the σ meson is not a universal exchange between any quark pair. The physical observed σ meson is an $u\bar{u}+d\bar{d}$

system which should not exchange between the $u(d)$ and s quarks. Only if one includes the hidden-color channel coupling can the chiral quark model accommodate a bound $N\Omega$ state. On the other hand, the QDCSM predicts there will be a bound $N\Omega$ state if the color singlet channel coupling is taken into account. The quark delocalization and color screening with the five color singlet channel coupling provides enough effective attraction to bound the $N\Omega$. Therefore, if experiment confirms the existence of the $N\Omega$ dibaryon state, bound or appearing as a D-wave resonance in $\Lambda - \Xi$ scattering, it will be a signal showing that the quark delocalization and color screening (an effective description of hidden-color channel coupling) is really responsible for the intermediate range attraction of baryon-baryon interaction. This mechanism is also preferred by the similarity between nuclear force and molecular force.

Experimental confirmation of the $N\Omega$ dibaryon will provide us the second sample of a six-quark system. It will provide another sample for the pursuit of low-energy scale QCD property and we hope there will be more experimental groups involved in the search for $N\Omega$ dibaryon with quantum numbers $SIJ^P = -3\frac{1}{2}2^+$.

ACKNOWLEDGMENT

This work is supported partly by the National Natural Science Foundation of China under Contracts No. 11175088, No. 11205091, and No. 11535005.

[1] F. J. Dyson and N. H. Xuong, Phys. Rev. Lett. **13**, 815 (1964).
[2] R. L. Jaffe, Phys. Rev. Lett. **38**, 195 (1977).
[3] R. L. Jaffe, Phys. Rep. **409**, 1 (2005); F. E. Close, Int. J. Mod. Phys. A **20**, 5156 (2005).
[4] T. Goldman, K. Maltman, G. J. Stephenson, K. E. Schmidt, and F. Wang, Phys. Rev. C **39**, 1889 (1989).
[5] M. Bashkanov *et al.* (CELSIUS-WASA Collaboration), Phys. Rev. Lett. **102**, 052301 (2009).
[6] P. Adlarson *et al.* (WASA-at-COSY Collaboration), Phys. Rev. Lett. **106**, 242302 (2011).
[7] P. Adlarson *et al.* (WASA-at-COSY Collaboration), Phys. Rev. Lett. **112**, 202301 (2014).
[8] F. Wang, J. L. Ping, G. H. Wu, L. J. Teng, and T. Goldman, Phys. Rev. C **51**, 3411 (1995).
[9] J. L. Ping, H. R. Pang, F. Wang, and T. Goldman, Phys. Rev. C **65**, 044003 (2002).
[10] J. L. Ping, H. X. Huang, H. R. Pang, F. Wang, and C. W. Wong, Phys. Rev. C **79**, 024001 (2009).
[11] M. Bashkanov, S. J. Brodsky, and H. Clement, Phys. Lett. B **727**, 438 (2013).
[12] Y. B. Dong, P. N. Shen, F. Huang, and Z. Y. Zhang, Phys. Rev. C **91**, 064002 (2015).
[13] A. Gal and H. Garcilazo, Phys. Rev. Lett. **111**, 172301 (2013).
[14] A. Gal and H. Garcilazo, Nucl. Phys. A **928**, 73 (2014).
[15] H. R. Pang, J. L. Ping, F. Wang, T. Goldman, and E. G. Zhao, Phys. Rev. C **69**, 065207 (2004).
[16] M. Chen, H. X. Huang, J. L. Ping, and F. Wang, Phys. Rev. C **83**, 015202 (2011).
[17] T. Goldman, K. Maltman, G. J. Stephenson, K. E. Schmidt, and F. Wang, Phys. Rev. Lett. **59**, 627 (1987).
[18] Q. B. Li and P. N. Shen, Eur. Phys. J. A **8**, 417 (2000).
[19] F. Etminan *et al.* (HAL Collaboration), Nucl. Phys. A **928**, 89 (2014).
[20] J. Yoshida *et al.*, in *International Workshop on Hadron Nuclear Physics* 2015, July 7–11, Krabi, Thailand, Book of Abstracts HNP2015, p. 39.
[21] N. Ishii, S. Aoki, and T. Hatsuda, Phys. Rev. Lett. **99**, 022001 (2007).
[22] C. Alexandrou, P. de Forcrand, and A. Tsapalis, Phys. Rev. D **65**, 054503 (2002); T. T. Takahashi, H. Suganuma, Y. Nemoto, and H. Matsufuru, *ibid.* **65**, 114509 (2002).
[23] F. Okiharu, H. Suganuma, and T. T. Takahashi, Phys. Rev. Lett. **94**, 192001 (2005).
[24] Y. Fujiwara, C. Nakamoto, and Y. Suzuki, Phys. Rev. Lett. **76**, 2242 (1996); Y. W. Yu, Z. Y. Zhang, P. N. Shen, and L. R. Dai, Phys. Rev. C **52**, 3393 (1995).
[25] A. Valcarce, H. Garcilazo, F. Fernández, and P. Gonzalez, Rep. Prog. Phys. **68**, 965 (2005), and references therein.
[26] M. Ablikim *et al.* (BES Collaboration), Phys. Lett. B **598**, 149 (2004).
[27] N. Kaiser, S. Grestendorfer, and W. Weise, Nucl. Phys. A **637**, 395 (1998); E. Oset, H. Toki, M. Mizobe, and T. T. Takahashi, Prog. Theo. Phys. **103**, 351 (2000); M. M. Kaskulov and H. Clement, Phys. Rev. C **70**, 014002 (2004).
[28] F. Wang, G. H. Wu, L. J. Teng, and T. Goldman, Phys. Rev. Lett. **69**, 2901 (1992); G. H. Wu, L. J. Teng, J. L. Ping, F. Wang, and T. Goldman, Phys. Rev. C **53**, 1161 (1996).
[29] J. L. Ping, F. Wang, and T. Goldman, Nucl. Phys. A **657**, 95 (1999); G. H. Wu, J. L. Ping, L. J. Teng *et al.*, *ibid.* **673**, 279 (2000); H. R. Pang, J. L. Ping, F. Wang, and T. Goldman, Phys. Rev. C **65**, 014003 (2001).
[30] L. Z. Chen, H. R. Pang, H. X. Huang, J. L. Ping, and F. Wang, Phys. Rev. C **76**, 014001 (2007).
[31] H. X. Huang, P. Xu, J. L. Ping, and F. Wang, Phys. Rev. C **84**, 064001 (2011).
[32] J. Vijande, F. Fernandez, and A. Valcarce, J. Phys. G **31**, 481 (2005).
[33] H. Garcilazo, T. Fernandez-Carames, and A. Valcarce, Phys. Rev. C **75**, 034002 (2007).
[34] Q. B. Li, P. N. Shen, Z. Y. Zhang, and Y. W. Yu, Nucl. Phys. A **683**, 487 (2001).
[35] M. Kamimura, Supp. Prog. Theo. Phys. **62**, 236 (1977).
[36] V. A. Babenko and N. M. Petrov, Phys. Atom. Nucl. **66**, 1319 (2003).